Asymmetric confinement for defining outgrowth directionality

Paul M. Holloway[1,2]*, Grace I. Hallinan[3]*, Manjunath Hegde[1], Simon I.R. Lane[4], Katrin Deinhardt[3] and Jonathan West[1†]

[1]Cancer Sciences, Faculty of Medicine, University of Southampton, UK.

[2]Investigative Medicine Division, Radcliffe Department of Medicine, University of Oxford, UK.

[3]Biological Sciences, Faculty of Environmental and Life Sciences, University of Southampton, UK.

[4]Faculty of Engineering and Physical Sciences, University of Southampton, UK.

* equal contribution

† corresponding author

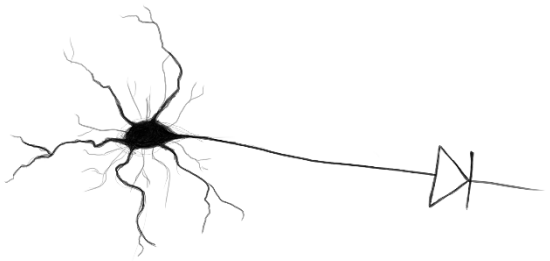

Edge-guidance and turning angle principles were used to design asymmetric microstructures to affect unidirectional outgrowth bias and provide new insights into pathfinding.

Abstract

Directional connectivity is required to develop accurate *in vitro* models of the nervous system. This research investigated the interaction of neuronal outgrowths with asymmetric microstructured geometries to provide insights into the mechanisms governing unidirectional outgrowth bias. The structures were designed using edge-guidance and critical turning angle principles to study different prohibitive to permissive edge-guidance ratios. The different structures enable outgrowth in the permissive direction, while reducing outgrowth in the prohibitive direction. Outgrowth bias was probabilistic in nature, requiring multiple structures for effective unidirectional bias in primary hippocampal cultures at 14 days *in vitro*. Arrowhead structures with acute posterior corners were optimal, enabling 100% unidirectional outgrowth bias by virtue of re-routing and delay effects.

Introduction

Directional connectivity is a hallmark of the functional anatomy of the nervous system and derives from the asymmetric localisation of materials within the dendritic and axonal sub-cellular compartments. Such ordered connectivity is inherent to the correct functioning of neuronal circuits, and underlies material propagation in disease, with notable examples being the retrograde transport of rabies virus and the anterograde spread of tau pathology in Alzheimer's disease. Investigations of such processes would benefit from *in vitro* models in which outgrowth orientation is defined.

Outgrowth specification is a developmental process, in which multiple neurites project from the cell body, one of which becomes programmed to be the emitter axon, with the remainder defaulting to dendrite receiver structures[1]. Thus a competitive outgrowth phenomena exists[2-4], with the neurite experiencing the most favourable cues destined to axon commitment. It is widely accepted that murine hippocampal axons are defined by substantial lengths, commonly >100 microns, whereas dendritic extensions are commonly limited to a few tens of microns[5, 6]. The pathfinding capabilities of growth cones provide a means to promote time-ensembled outgrowth in a desired (permissive) direction.

Conceptually, axon specification can be directed using asymmetric environmental cues to promote outgrowth from one neuron while the same cues, encountered from the opposite direction prohibit outgrowth from a second neuron. Consequently the first neuron develops an axon that interfaces to the dendrite of the second. Evidence from experiments using microfabricated neuronal culture environments reveals remarkable edge-finding capabilities of neuritic growth cones, able to circumnavigate 20-μm-diameter pillars[7]. This invites the possibility to use asymmetric geometries to preference outgrowth directionality.

Complex optical[8], electrokinetic[9] and microfluidic[10] active methods have been developed for directing outgrowths. Alternatively, passive methods comprising microchannels[7, 11-14] and material micropatterns[15-20] that do not require instrumentation can be used. Planar material micropatterns involving cell adhesion areas surrounded by cell repellent areas generally produce short-lived pattern fidelity due to microenvironment remodelling by the outgrowth and also the tendency of outgrowths to 'jump' cell repellent surfaces. Instead, microchannels can be used to confine outgrowth throughout the duration of culture and are therefore the focus of this study. To impart directionality several asymmetric confinement strategies have been investigated. These have adopted the parallel culture compartments pioneered by Taylor[11] that are interfaced via numerous sub-cellular-scale outgrowth channels. Outgrowth channels have been developed that abruptly taper from a wide inlet permissive for growth cone entry to a narrow outlet that limits entry[21, 22]. Outgrowth channels have been developed that abruptly taper from a wide inlet permissive for growth cone entry to a narrow outlet that limits entry[21, 22]. More recently Renault *et al* implemented more effective loop-back structures that build on the observation that outgrowths cannot be redirected beyond a critical angle. This approach employed repeat motifs to achieve a cumulative outgrowth bias[23]. Similarly, repeated arrow-shaped motifs, also used by the planar micropatterning community[24-26] , or barbed channel indentations[27], have been used to direct outgrowth and produce a functionally orientated synaptic interface.[28]

This study aims to further our understanding of the nature of outgrowth pathfinding during asymmetric confinement. Based on the prohibitive angle observation a series of asymmetric geometries termed arch, pretzel, heart and arrowheads were designed and used to investigate permissive:prohibitive edge ratios (see Fig. 1). The precisely fabricated microstructures deliver reproducible outgrowth data to determine state of the art performance and provide insights into the underlying mechanisms defining outgrowth pathfinding.

Concept

Outgrowth edge guidance is frequently observed on both planar patterned substrates and in microchannels. In these environments, the growth cone arrives at the interface to a non-permissive area, either a cell repellent coating or a physical wall, where the outgrowth is re-directed along the interface. In contrast, outgrowth re-routing away from non-permissive areas is a costly behaviour in terms of energy and time and is seldom seen. The growth cone does however deviate from edge guidance when abrupt directional changes are imparted. Francisco *et al* documented outgrowth cornering, with the probability of cornering decreasing as the deviation angle increased to 135°.[29] Taking this further, Renault *et al* used edge directional changes in expansive regions to demonstrate trajectory continuation, not edge guidance, at progressively larger turning angles (≥84°)[23], a characteristic attributed to the non-zero bending stiffness of outgrowths.[30, 31] With this understanding Renault *et al* developed arch-shaped structures comprising multiple linear paths joined by loops[23] (see Fig. 1). Channel intersections introduce directional asymmetry with oblique turning angles that return outgrowths to the emitter culture and acute turning angles that are neglected to produce a continuous outgrowth trajectory towards the receiver culture compartment. In essence a 'permissive' direction produces a linear outgrowth trajectory, whereas the 'prohibitive' direction introduces a 1:1 probability of continuation or reversal. With multiple loop motifs, unidirectional outgrowth bias was demonstrated.

The requirement for multiple arch motifs indicates a probabilistic component to directional bias in these channel arrangements. Using this as a point of entry we developed a range of confined and open space asymmetric structures to investigate edge-guidance probabilities obeying the critical angle turning criteria (Fig. 1). Confined, microchannel structures termed arch and pretzel were designed. The arch is equivalent to the structure reported by Renault *et al*, that we predict has a prohibitive:permissive routing ratio of 1:1 in the undesired direction. The complex paths within the pretzel structure increase the theoretical routing ratio to 8:1. Taking this further we also developed open space asymmetric structures, termed heart and arrowhead. These involve expansive areas with perimeters fulfilling the critical turning angle criteria to allow an infinite prohibitive:permissive routing ratio to be investigated. The heart structures provide mirrored large radius of curvature paths for growth cone re-routing, whereas the arrowhead structures provide an acute corner, representing a minimal radius of curvature, and are predicted to delay, not re-route, outgrowths.

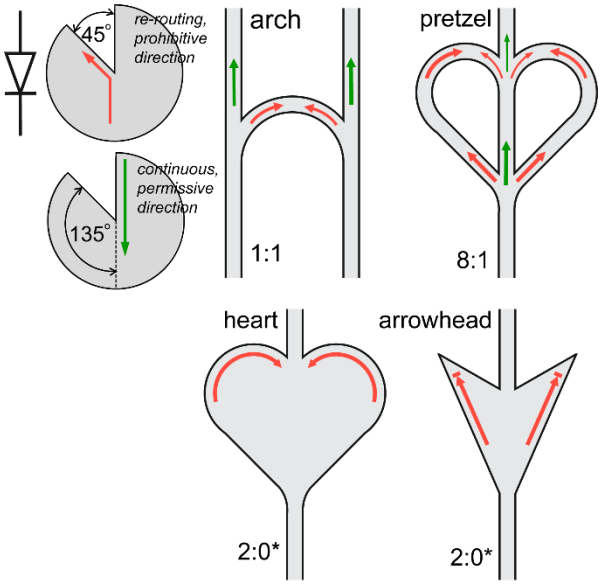

Figure 1. Illustration of predicted edge-guidance and critical angle effects re-routing outgrowths away from the axonal compartment (red, prohibitive direction) and enabling continuous outgrowths towards the axonal compartment (green, permissive direction). The asymmetric confinement structures with red arrows indicating prohibitive edge guidance paths and green arrows indicating permissive edge guidance paths in the 'prohibitive' direction. The prohibitive:permissive path ratios are quoted with the assumption (*) that edge guidance is required to traverse the structure.

Materials and Methods

Full details of the materials and methods used in this study are available in the on-line supplementary information. In brief, dual layer fabrication was used for moulding PDMS neuronal compartments interconnected using 800-μm-long outgrowth channels. To bias outgrowth directionality these incorporated asymmetric structures involving the 135° critical turning angle. Hippocampal neurons were isolated from embryonic day 15–18 C57BL/6 mouse brains and cultured in the microfluidic compartments for 14 days *in vitro* (DIV). Outgrowths were stained for βIII tubulin to assess outgrowth polarisation by fluorescent imaging. Data is plotted as motif (arch, pretzel, heart, arrowhead) number versus axonal projection (intensity levels of outgrowths that have traversed the inter-compartment distance at 14DIV). Differential interference contrast live imaging was used to observe outgrowth dynamics during asymmetric confinement.

Results and Discussion

Probabilistic edge-guidance

Outgrowths confined by the arch structures produced results consistent with the findings of Renault *et al*,[23] restricting outgrowth in the prohibitive direction while not significantly (minimally) affecting outgrowth in the permissive direction over the 14DIV period. Five arch motifs limited outgrowth in the prohibitive direction to 23% of the controls. The first arch motif results in re-direction probabilities described by the 1:1 ratio, after which the arch motifs have progressively reduced impact. We interpret the behaviour at the latter motifs results from the interconnected channel network, allowing initially

returned outgrowths to encounter other, linear outgrowths that act as a preferred scaffold for outgrowth guidance in either direction. Plotted in Fig. 2(B) this changes the prohibitive:permissive ratio to 1:3. Theoretical results at motifs 3–5 are consistent with experimental results at 14DIV, a duration necessary for the formation of mature, functional synapses.[32-34] Renault *et al* documented improved directional selectivity (90% v 10%) with only 3 motifs at 8DIV, a duration sufficient to see the emergence of outgrowths in the permissive direction across a tract of 800 μm. However, the additional travel distance associated with each loop motif (94 μm) reduces outgrowths exiting the microchannels in the prohibitive direction at this early time point.

The pretzel structures do not interconnect with neighbouring channels and with 8-fold edge-directed probabilistic bias we predicted improved unidirectional outgrowth. The level of outgrowths exiting via the prohibitive route reduced with each motif and by five motifs were limited to 10% compared to controls (with equivalent edge lengths), an improvement over the 23% observed with the arch motifs. However, these levels of outgrowth bias cannot be interpreted using simple probability theory (see Fig. 1). Closer inspection of an outgrowth exploring a pretzel structure in the prohibitive direction using live imaging documents branching, retraction, stalling and re-routing. Branching phenomena at channel intersections bypasses the edge-guidance probability behaviour we predicted. The observed behaviours implicate localised crosstalk within the molecular dynamics of outgrowth extension and retraction that ultimately determine trajectory. Importantly, this allows exploration of the majority of the pretzel structure before escape (Movie SI1). In this example, exploration by collateral branching produced a 16-hour dwell time. At the later 37–40 hour time points, retraction occurred (Movie SI2). We speculate that these delays may introduce a competitive advantage to other branches from the same axon outside the microchannel at the expense of the delayed outgrowth segment. In addition, the complex paths within the pretzel structure coupled with branching and retraction may lead to re-routing to the emitter culture.

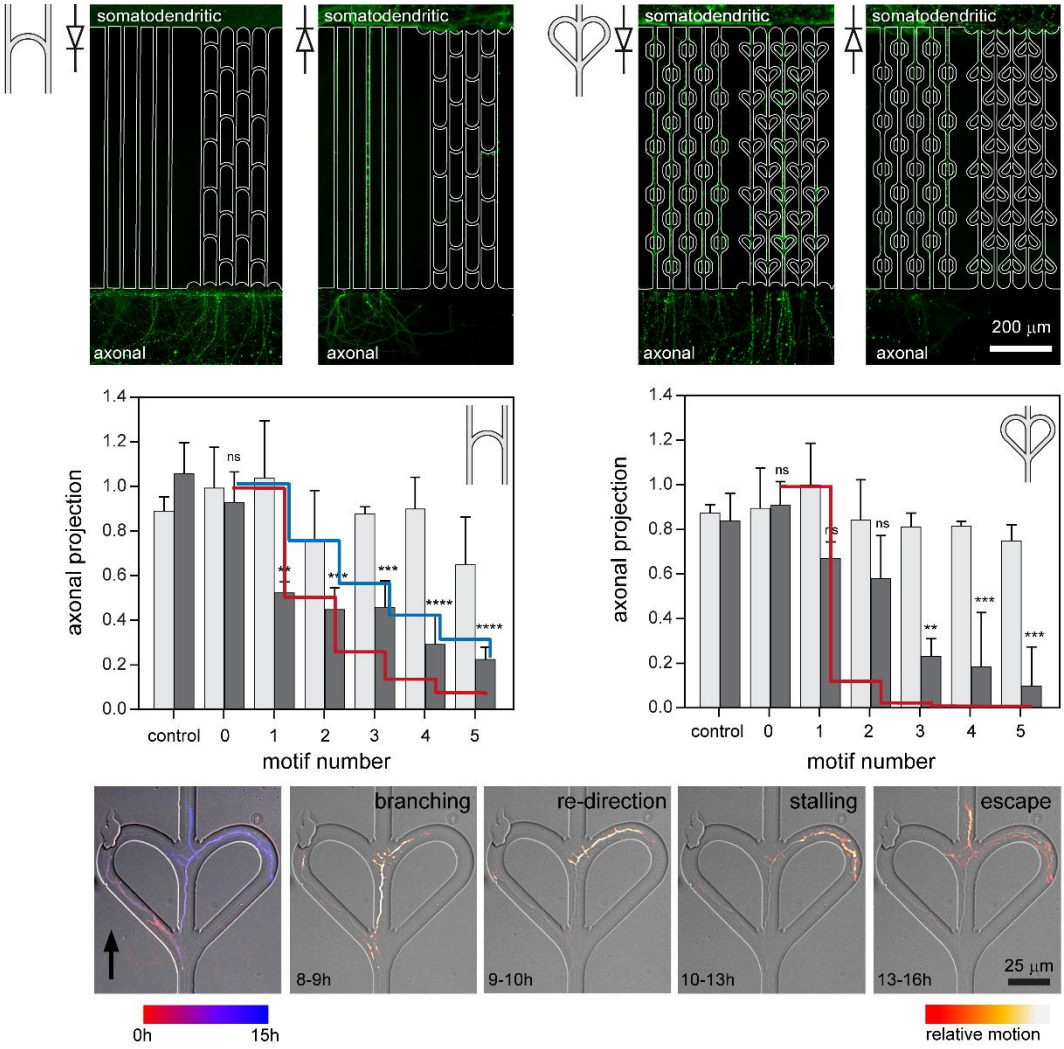

Figure 2. Comparison of 14DIV outgrowth levels during confinement in arch and pretzel microstructures in the permissive and prohibitive directions. Microchannels with asymmetric structures neighbouring control channels are used to best illustrate outgrowth behaviour. Outgrowths are stained for βIII tubulin. Larger field of view images are available in the SI Fig. 1 along with time-lapse footage (Movie SI1 and Movie SI2). Mean and standard deviation in the permissive direction (light grey) and prohibitive direction (dark grey) are plotted for arch and pretzel confinement devices. Levels for motif repeats were compared to controls using a *post hoc* one-way ANOVA (**p>0.01, ***p>0.001, ****p>0.0001; *n*=3). Projection is not significantly affected in the permissive direction in all cases. Probabilities are overlaid to describe the theoretical 1:1 arch edge-guidance ratio (red), the posited, cumulative 1:3 ratio (blue) and the theoretical 8:1 ratio (red) implicated in pretzel edge-guidance. DIC live image frame stacks documenting outgrowth dynamics within a pretzel structure. Arrow denotes direction of entry.

Open space delay structures

The heart and arrowhead asymmetric structures were designed with a theoretically infinite (2:0) prohibitive: permissive ratio, achieved by removing the continuous linear path. These structures also introduced directional bias given the edge finding and critical angle phenomena described by Renault *et al*, without significantly disturbing outgrowth in the permissive direction. Again, cumulative effects were observed with outgrowth levels in the prohibitive direction progressively reduced with each additional motif (Figure 3). In experiments involving 3 independent cell preparations, the mean axonal projection confined by five heart motifs was reduced to 22% of controls (equivalent to five arch motifs). In comparison, no axons projected into the opposing compartment for each replicate when traversing

five arrowhead motifs. The arrowheads therefore demonstrate superior unidirectional outgrowth guidance compared to the other asymmetric structures. Multiple barbed structures, with each barb representing half of an arrowhead structure, have also been used to enhance unidirectional outgrowth. However, with ten barbs on each side, a 4 week outgrowth duration was required to span the 800 μm inter-compartment distance[27], demonstrating that additional motifs are not necessarily more efficient for biased unidirectional outgrowth.

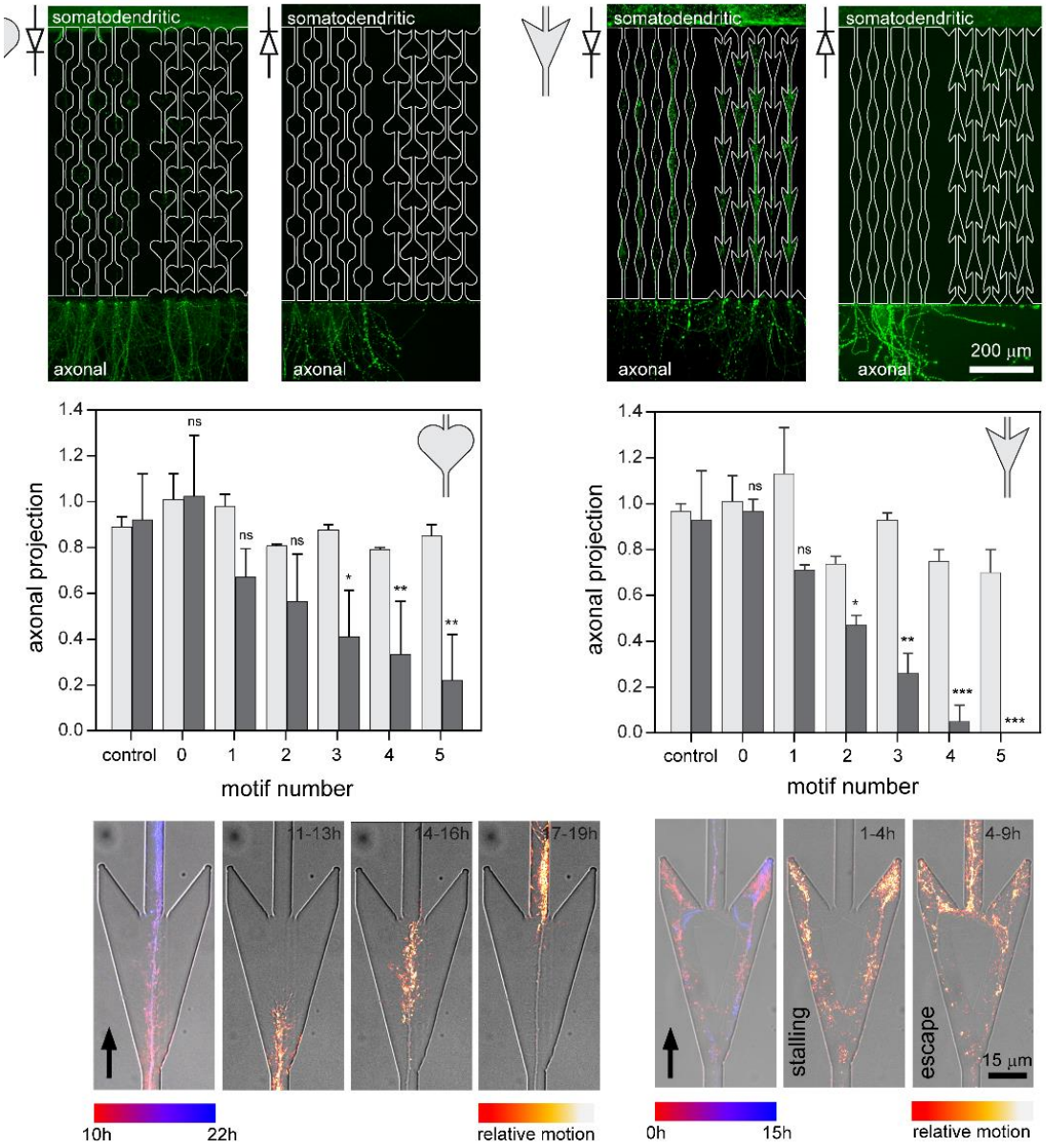

Figure 3. Comparison of 14DIV outgrowth levels during confinement in heart and arrowhead microstructures in the permissive and prohibitive directions. Microchannels with asymmetric structures neighbouring control channels are used to best illustrate outgrowth behaviour. Outgrowths are stained for βIII tubulin. Larger field of view images are available in the SI Fig. 2 along with time-lapse footage (Movie SI3 and Movie SI4). Mean and standard deviation in the permissive direction (light grey) and prohibitive direction (dark grey) are plotted for heart and arrowhead confinement devices. Levels for motif repeats were compared to controls using a one-way ANOVA (*p>0.1, **p>0.01, ***p>0.001; *n*=3). Projection is not significantly affected in the permissive direction in all cases. DIC live image frame stacks documenting outgrowth dynamics within arrowhead structures. Arrow denotes direction of entry.

The requirement for multiple motifs to achieve directional bias indicates that edge-guidance and the critical turning angle are not the defining determinants of pathfinding within the infinite

prohibitive:permissive routing ratio heart and arrowhead microstructures. Indeed, we have observed a growth cone U-turn in the constricted (7.5-μm-wide), straight channel regions. In addition, we speculate that the reduced unidirectional bias in the heart structures results from outgrowth guidance to the centre of the heart structure where there is adequate space for remodelling to locate the exit.

To provide insights into the highly efficient unidirectional bias in the arrowhead structures live imaging was applied (figure 3): In one instance, consistent with observations by Francisco *et al* who used abruptly expanding microchannels[29], the growth cone enlarges as the arrowhead broadens. Routing was no-longer governed by edge-guidance such that the outgrowth rapidly (6 hours) traversed and escaped the structure (Movie SI3). In another example, the outgrowth branched with two growth cones becoming confined within each acute corner described by the posterior arrowhead tips. By remodelling, another branch was initiated with the new growth cone overcoming the 135° critical turning angle by producing a Z-shaped morphology with surprisingly tight, 2 μm, radii of curvature introduced at >90° corners that allow the outgrowth to escape the arrowhead structure (Movie SI4). Of note, the imaged arrowhead was a rare example of depression in the central region, excluding outgrowth access, thus removing this path for re-routing the outgrowth to the emitter culture. Nevertheless this evidence documents initial growth cone stalling within the acute corners defining the posterior arrowhead tips. This indicates that progressive confinement provides an effective outgrowth delay cue.

The superior performance of the arrowhead structures also corroborates the enhanced unidirectional connectivity bias demonstrated by Gladkov *et al* using triangular structures (especially "horn traps") funnelling to narrow exits[32], by le Feber *et al* using channels with internal barbed structures[27] and possibly by Hattori *et al* who uniquely used an asymmetric surface topography[35]. The generalised findings from this and other research[23, 27, 29, 32] indicate that the optimal geometry will maximise outgrowth delay by a combination of asymmetry involving edge-guidance, the critical turning angle and progressive confinement by cul-de-sac, or dead-end features. Consequently, outgrowths, branch down-stream, re-routing into the somatodendritic compartment, or do not achieve specification to enable other outgrowths within the somatodendritic compartment to become axons.

Conclusions

Asymmetric microstructures obeying a critical turning angle were used to investigate edge-guidance based outgrowth pathfinding with a view to determine optimal structures for unidirectional outgrowth that are required for polarised connectivity. The complex mechanisms enabling outgrowth navigation during asymmetric confinement produce directional bias. In particular, branching, causes deviation from simple probability theory. Instead, the results provide evidence advocating the use of acute corners (arrowhead) or complex paths (pretzel) to effect both outgrowth delay and re-routing in contrast to structures that only effect re-routing (arch and heart). The research also lends weight to the use of microfabricated structures as a means to precisely dissect pathfinding mechanisms, and also informs the design of future structures with enhanced unidirectional outgrowth bias. The availability of more efficient structures will enable the design of more compact polarised neuronal co-cultures, paving the way for a range of applications, including the development of compound screening platforms, precisely defined neuronal circuitry and potentially resorbable scaffolds for nerve regeneration or transplantation.

Acknowledgements

The research was funded by a Higher Education Innovation Fund (PMH), Alzheimer's Research UK (ARUK-PhD2014-10 and ARUK-PPG2017B-001, GIH and KD) and an Institute for Life Sciences fellowship (JW).

References

1. M. Stiess and F. Bradke, *Dev Neurobiol*, 2011, **71**, 430-444.
2. Z. D. Wissner-Gross, M. A. Scott, D. Ku, P. Ramaswamy and M. Fatih Yanik, *Integr Biol (Camb)*, 2011, **3**, 65-74.
3. C. G. Dotti and G. A. Banker, *Nature*, 1987, **330**, 254.
4. K. Goslin and G. Banker, *The Journal of Cell Biology*, 1989, **108**, 1507-1516.
5. A. Yamada, M. Vignes, C. Bureau, A. Mamane, B. Venzac, S. Descroix, J.-L. Viovy, C. Villard, J.-M. Peyrin and L. Malaquin, *Lab on a Chip*, 2016, **16**, 2059-2068.
6. Z. Lei, Y. Ruan, A. N. Yang and Z. C. Xu, *Neuroscience Letters*, 2006, **407**, 224-229.
7. N. D. Dinh, Y. Y. Chiang, H. Hardelauf, J. Baumann, E. Jackson, S. Waide, J. Sisnaiske, J. P. Frimat, C. van Thriel, D. Janasek, J. M. Peyrin and J. West, *Lab Chip*, 2013, **13**, 1402-1412.
8. A. Ehrlicher, T. Betz, B. Stuhrmann, D. Koch, V. Milner, M. G. Raizen and J. Käs, *Proceedings of the National Academy of Sciences*, 2002, **99**, 16024-16028.
9. T. Honegger, M. A. Scott, M. F. Yanik and J. Voldman, *Lab on a Chip*, 2013, **13**, 589-598.
10. H. Dermutz, R. R. Gruter, A. M. Truong, L. Demko, J. Voros and T. Zambelli, *Langmuir*, 2014, **30**, 7037-7046.
11. A. M. Taylor, S. W. Rhee, C. H. Tu, D. H. Cribbs, C. W. Cotman and N. L. Jeon, *Langmuir : the ACS journal of surfaces and colloids*, 2003, **19**, 1551-1556.
12. A. M. Taylor, M. Blurton-Jones, S. W. Rhee, D. H. Cribbs, C. W. Cotman and N. L. Jeon, *Nature Methods*, 2005, **2**, 599.
13. P. Shi, M. A. Scott, B. Ghosh, D. Wan, Z. Wissner-Gross, R. Mazitschek, S. J. Haggarty and M. F. Yanik, *Nature Communications*, 2011, **2**, 510.
14. A. Kunze, R. Meissner, S. Brando and P. Renaud, *Biotechnology and Bioengineering*, 2011, **108**, 2241-2245.
15. D. Kleinfeld, K. Kahler and P. Hockberger, *The Journal of Neuroscience*, 1988, **8**, 4098-4120.
16. B. C. Wheeler, J. M. Corey, G. J. Brewer and D. W. Branch, *Journal of Biomechanical Engineering*, 1999, **121**, 73-78.
17. A. K. Vogt, L. Lauer, W. Knoll and A. Offenhäusser, *Biotechnology Progress*, 2003, **19**, 1562-1568.
18. J. P. Frimat, J. Sisnaiske, S. Subbiah, H. Menne, P. Godoy, P. Lampen, M. Leist, J. Franzke, J. G. Hengstler, C. van Thriel and J. West, *Lab Chip*, 2010, **10**, 701-709.
19. H. Hardelauf, J. Sisnaiske, A. A. Taghipour-Anvari, P. Jacob, E. Drabiniok, U. Marggraf, J. P. Frimat, J. G. Hengstler, A. Neyer, C. van Thriel and J. West, *Lab Chip*, 2011, **11**, 2763-2771.
20. H. Hardelauf, S. Waide, J. Sisnaiske, P. Jacob, V. Hausherr, N. Schobel, D. Janasek, C. van Thriel and J. West, *Analyst*, 2014, **139**, 3256-3264.

21. J. M. Peyrin, B. Deleglise, L. Saias, M. Vignes, P. Gougis, S. Magnifico, S. Betuing, M. Pietri, J. Caboche, P. Vanhoutte, J. L. Viovy and B. Brugg, *Lab Chip*, 2011, **11**, 3663-3673.

22. R. Renault, N. Sukenik, S. Descroix, L. Malaquin, J. L. Viovy, J. M. Peyrin, S. Bottani, P. Monceau, E. Moses and M. Vignes, *PLoS One*, 2015, **10**, e0120680.

23. R. Renault, J. B. Durand, J. L. Viovy and C. Villard, *Lab Chip*, 2016, **16**, 2188-2191.

24. M. A. Scott, Z. D. Wissner-Gross and M. F. Yanik, *Lab Chip*, 2012, **12**, 2265-2276.

25. O. Feinerman, A. Rotem and E. Moses, *Nature Physics*, 2008, **4**, 967.

26. J. Albers and A. Offenhäusser, *Frontiers in bioengineering and biotechnology*, 2016, **4**, 46-46.

27. J. le Feber, W. Postma, E. de Weerd, M. Weusthof and W. L. C. Rutten, *Frontiers in neuroscience*, 2015, **9**, 412-412.

28. A. Gladkov, Y. Pigareva, D. Kutyina, V. Kolpakov, A. Bukatin, I. Mukhina, V. Kazantsev and A. Pimashkin, *Scientific Reports*, 2017, **7**, 15625.

29. H. Francisco, B. B. Yellen, D. S. Halverson, G. Friedman and G. Gallo, *Biomaterials*, 2007, **28**, 3398-3407.

30. S. Roth, G. Bugnicourt, M. Bisbal, S. Gory-Fauré, J. Brocard and C. Villard, *Small*, 2012, **8**, 671-675.

31. R. M. Smeal, R. Rabbitt, R. Biran and P. A. Tresco, *Annals of Biomedical Engineering*, 2005, **33**, 376-382.

32. A. Gladkov, Y. Pigareva, D. Kutyina, V. Kolpakov, A. Bukatin, I. Mukhina, V. Kazantsev and A. Pimashkin, *Sci Rep*, 2017, **7**, 15625.

33. M. Ichikawa, K. Muramoto, K. Kobayashi, M. Kawahara and Y. Kuroda, *Neuroscience Research*, 1993, **16**, 95-103.

34. T. Basarsky, V. Parpura and P. Haydon, *The Journal of Neuroscience*, 1994, **14**, 6402-6411.

35. S. Hattori, J. Suzurikawa, R. Kanzaki, Y. Jimbo, T. Hamaguchi, H. Takahashi and M. Nakao, *Electronics and Communications in Japan*, 2010, **93**, 17-25.